

Pressure and temperature dependence of viscosity and diffusion coefficients of a glassy binary mixture

Arnab Mukherjee, Sarika Bhattacharyya, and Biman Bagchi^{a)}

Solid State and Structural Chemistry Unit, Indian Institute of Science, Bangalore -12, India

Extensive isothermal-isobaric (NPT) molecular dynamics simulations at many different temperatures and pressures have been carried out in the well-known Kob–Andersen binary mixture model to monitor the effect of pressure (P) and temperature (T) on the dynamic properties such as the viscosity (η) and the self-diffusion (D_i) coefficients of the binary system. The following results have been obtained: (i) Compared to temperature, pressure is found to have a weaker effect on the dynamical properties. Viscosity and diffusion coefficients are found to vary *exponentially* with pressure up to a certain high pressure after which the nature of exponential dependence changes. This change is rather sharp. (ii) With temperature, on the other hand, both viscosity and diffusion show super-Arrhenius dependence. Viscosity and diffusion coefficients fit well also to the mode coupling theory (MCT) prediction of a power law dependence on the temperature. The MCT critical temperature (T_c) for both the two dynamical properties are significantly higher than the corresponding critical temperature T_0^η obtained by fitting to the Vogel–Fulcher–Tammann (VFT) equation. (iii) The critical temperature for viscosity (T_0^η) is considerably larger than that for the diffusion coefficients ($T_0^{D_i}$) implying the decoupling between diffusion and viscosity in deeply supercooled liquid. (iv) The nature of the motion of small particles change from continuous to hopping dominated once the larger ones are frozen. (v) The potential energy of the system shows a minimum against density at a relatively high density when the latter is changed by applying pressure at a constant temperature.

I. INTRODUCTION

Dynamics in supercooled liquid has remained one of the most inquisitive but obscure subjects of recent scientific interest. Dramatic slowing down of dynamics from normal to supercooled liquid has attracted an enormous number of studies in the supercooled liquid regime.^{1,2} Many anomalies in supercooled liquid arise from an interplay between the different dynamical cooperativity in different regions.³ Temperature dependence of η categorizes a system directly to strong or fragile according to the dependence being Arrhenius or super-Arrhenius. The concept of fragility is often connected to the free energy landscape, configurational entropy and hopping dynamics.^{4–6} In contrast, the pressure dependence of transport properties has drawn much less attention than their temperature dependence. Answers to many questions regarding pressure dependence are either not known or ill-understood. For example, viscosity is known to show an exponential dependence on the pressure in the normal liquid state. What happens to this dependence as the glass transition is approached? What is the correlation between the pressure and the temperature dependence of viscosity and diffusion? We are not aware that these questions have been answered satisfactorily yet.

In this work, extensive NPT molecular dynamics (MD) simulations have been carried out on the well-known Kob–Andersen model^{7,8} by varying both the temperature and the

pressure of the system. The advantage of Kob–Andersen model is that it is not only a simple model system, but it does not form a crystalline state, thus detailed simulations can safely be carried out. Although there have been several studies on this particular system in the past,^{6–13} no detailed investigations of the effects of pressure on the dynamic properties of the system seems to have been carried out—most studies focused on the temperature dependence. The non-Arrhenius temperature dependence of inverse diffusivity obtained earlier⁶ suggests that the above model is a weakly fragile model according to Angell fragility concept.¹⁴

The pressure dependence of the dynamical properties η and D_i is found to be weaker than the temperature dependence. η and D_i vary exponentially with pressure. But after a certain high pressure, there is a clear break in the strength of exponentiality, i.e., there is a change in slope of $\ln(\eta)$ against pressure. This change is rather sharp and we have discussed the probable origin of this change. The relatively weak pressure dependence has been analyzed from a different angle by plotting η against density (ρ) where density has been changed by varying pressure at two different temperatures. We find that variation in η with ρ is significantly large if the temperature is low. Otherwise, at high temperature, the density dependence of dynamical properties (η and D) is surprisingly weak.

Mode coupling theory seems to work for a large range of temperature variation of η and D_i . The power law dependence of viscosity [$\eta = C_\eta^* (T - T_c^\eta)^{-\gamma_\eta}$] and diffusion coefficients [$D_i = C_{D_i}^* (T - T_c^{D_i})^{\gamma_{D_i}}$] agree reasonably well

^{a)}Electronic mail: bbagchi@sscu.iisc.ernet.in

with the simulation results except for viscosity at high temperature where the agreement is weak. On the other hand, the critical temperatures, both T_c^η and $T_c^{D_i}$ obtained from MCT is higher than those obtained from the VFT fitting. MCT seems to breakdown in deeply supercooled liquid region well before the glass transition. VFT also estimates a higher critical temperature value for viscosity when compared to those of diffusion coefficients. This supports the observed deviation from the well-known Stokes–Einstein law in the proximity of the glass transition temperature.^{15–18} Both VFT and MCT predict higher critical temperature of diffusion for the bigger particles than that of smaller ones. This implies that the smaller particles remain mobile even when bigger particles are almost frozen.

One of the main motivations of the present study is to inquire about the presence of any dynamic signature of the crossover from diffusive to the free energy landscape dominated regime in the macroscopic transport properties (aside from the well-known hopping), such as viscosity and diffusion. We found that both these two transport properties show a remarkable change in their dependence on pressure. This change seems to indicate some changes in the mechanism of the transport processes. A sharp change in the time correlation function of the stress of the system is noticed at low temperatures and high pressures. The simulations also find the emergence of a power law like behavior in the intermediate time decay of the stress time correlation function at the lowest temperature simulated.

Arrangement of the rest of the paper is as follows. Basic definitions of viscosity and diffusion coefficients and the details of simulation are given in Sec. II. Section III contains the detailed discussion and the results of temperature and pressure dependence of diffusion coefficients and viscosity. Moreover, some of the static properties have also been discussed here. In Sec. IV, the emergence of hopping dynamics in the supercooled liquid region is discussed. Section V is dedicated to the discussion on the nonexponential nature of stress relaxation in the supercooled liquid. Finally, we conclude the paper in Sec. VI with a brief discussion.

II. BASIC DEFINITIONS AND DETAILS OF SIMULATION

Viscosity is calculated according to the microscopic expression formulated in terms of stress autocorrelation function, given by^{19,20}

$$\eta(t) = (Vk_B T)^{-1} \langle \sigma^{\alpha\beta}(0) \sigma^{\alpha\beta}(t) \rangle, \quad (1)$$

where $\alpha \neq \beta = x, y, z$ and $\sigma^{\alpha\beta}$ is the off-diagonal element of the stress tensor, given by

$$\sigma^{\alpha\beta} = \sum_{j=1}^N [(p_j^\alpha p_j^\beta / m) + F_j^\beta \alpha_j], \quad (2)$$

where F_j^β is the β -component of the force acting on the j th particle and the corresponding position of the j th particle is α_j , p_j^α is the α -component of the momentum of j th particle, m being the mass of the particle. Among total N number of particles present in the system, N_1 are solvent particles N_2 are solute particles, where $N_1 + N_2 = N$.

Frequency dependent viscosity is obtained by Laplace transforming $\eta(t)$

$$\eta(z) = \int_0^\infty dt \exp(-zt) \eta(t). \quad (3)$$

Macroscopic viscosity is the zero frequency limit of $\eta(z)$.

The self-diffusion coefficient, on the other hand, is the property of a single tagged particle. It can be obtained from mean square displacement (MSD) and is formulated by Einstein as

$$D_i = \lim_{t \rightarrow \infty} \frac{1}{6t} \langle |\mathbf{r}_i(t) - \mathbf{r}_i(0)|^2 \rangle. \quad (4)$$

Another way of calculating diffusion coefficient is from velocity autocorrelation function (VACF),²¹

$$D_i = \frac{1}{3} \int_0^\infty dt \langle \mathbf{v}_i(0) \cdot \mathbf{v}_i(t) \rangle, \quad (5)$$

where \mathbf{v}_i is the velocity of the i th particle. However, the VACF approach is not a numerically viable method to calculate the diffusion coefficient values in the supercooled liquid region.²² So, we mainly calculated diffusion coefficients from MSD.

We have carried out a series of very long molecular dynamic simulations at constant pressure (P), temperature (T) and constant total number of particles (N)^{23–25} in the Kob–Andersen model⁷ of binary mixtures which is well-known as a good glass former. We have taken a set of total 500 particles (solvent A + solute B particles) with 0.2 solute composition. The particles interact via a modified Lennard-Jones potential which sets a cutoff radius r_c outside which, the potential energy is 0. The particular form of the potential is given by²⁶

$$U_{ij} = 4\epsilon_{ij} \left\{ \left[\left(\frac{\sigma_{ij}}{r_{ij}} \right)^{12} - \left(\frac{\sigma_{ij}}{r_{ij}} \right)^6 \right] + \left[6 \left(\frac{\sigma_{ij}}{r_c} \right)^{12} - 3 \left(\frac{\sigma_{ij}}{r_c} \right)^6 \right] (r/r_c)^2 - 7 \left(\frac{\sigma_{ij}}{r_c} \right)^{12} + 4 \left(\frac{\sigma_{ij}}{r_c} \right)^6 \right\}, \quad (6)$$

where the cutoff distance r_c in this particular case has been taken as equal to 2.5σ . Use of above potential form takes care of the fact that both potential and force are continuous at the cutoff distance. i and j denote two different particles. Sizes of the particles are $\sigma_{AA} = 1.0\sigma$, $\sigma_{BB} = 0.88\sigma$, $\sigma_{AB} = 0.8\sigma$. The two different particles are more attractive than the similar ones. $\epsilon_{AA} = 1.0\epsilon$, $\epsilon_{BB} = 0.5\epsilon$, $\epsilon_{AB} = 1.5\epsilon$. Masses of the two different particles are same, i.e., $m_A = m_B = 1.0$. All distances and interaction energies are scaled by the bigger solvent parameters (σ_{AA} and ϵ_{AA}).

To study the temperature dependence of the above system, we have varied reduced temperature T^* ($k_B T / \epsilon$) from 0.6 to 2.0 keeping the reduced pressure P^* (ϵ / σ^3) constant at 10.0. On the other hand, the pressure variation studies were performed at two different constant temperatures. At $T^* = 1.0$, P^* is varied from 2.5 to 25.0 and the second study was done at $T^* = 0.5$ varying P^* from 0.5 to 4.5. Pressure is kept constant by Anderson's piston method while, in the case of temperature, a damped oscillator method has been adopted

which keeps temperature constant at each and every step.²³ The piston mass involved here is $0.0027(m/\sigma^4)$ which is regarded as optimum.²³

In each case, three different initial configurations were taken to calculate the viscosity and diffusion coefficients. Diffusion coefficients are calculated from both velocity autocorrelation function and mean square displacement. But in the relatively supercooled liquid region, diffusion coefficients have been calculated from mean square displacement for the reason stated earlier. Viscosity is calculated from the integration of the stress correlation given by Eq. (1). Three different off-diagonal stress correlations have been calculated from a single run and taken an average over them for each of the three data set. Thus viscosity is obtained from the average over nine data sets.

Relatively smaller time step $0.001 \tau (m_A \sigma_{AA}^2 / k_B T)$ has been employed. System equilibration is varied depending upon the temperature and pressure of the system from 2×10^5 to 15×10^5 steps and data collection steps varied from 2×10^6 to 15×10^6 .

III. RESULTS AND DISCUSSION

Supercooled liquids exhibit many interesting static and dynamic properties. In the following subsections, we present our simulation results.

A. Radial distribution function

In Figs. 1(a) and 1(b), we plot all the three partial radial distribution functions $g_{AA}(r)$, $g_{AB}(r)$, $g_{BB}(r)$ of the Kob–Andersen model for $P^* = 2.5(\epsilon_{AA}/\sigma_{AA}^3)$ and $P^* = 25.0(\epsilon_{AA}/\sigma_{AA}^3)$. We see a splitting of the second peak of $g_{AA}(r)$ and $g_{AB}(r)$ at high pressure which is known to be the characteristic signature of dense random packing.²² The structure of $g_{BB}(r)$ is interesting. It has an insignificant first peak which originates from the least interactions between the B type of particles. The second peak of $g_{BB}(r)$ is higher than that of the first peak signifying that the predominant B–B correlation takes place at the second coordination shell. This second peak also splits in the high pressure region as seen in Fig. 1(b). The last is an interesting result, showing correlations with the second shell.

B. Temperature dependence of viscosity

We plot temperature dependence of viscosity (η) in Fig. 2(a). This figure clearly shows a super-Arrhenius behavior of viscosity when $\ln(\eta)$ is plotted against the inverse of temperature ($1/T^*$). This super-Arrhenius behavior classifies the Kob–Andersen model into a fragile liquid, according to Angell fragility concept. However, the fragility is weak, as observed by Sastry.⁶ As the viscosity shows the super-Arrhenius kind of behavior, we try to fit η to the Vogel–Fulcher–Tammann (VFT) type of equation as below,

$$\eta = A_\eta \times \exp[E_\eta / (T - T_0^\eta)], \quad (7)$$

where T_0^η is the critical temperature where η diverges. Figure 2(b) shows the nice fit of $\ln(\eta)$ against $(1/T - T_0^\eta)$ where T_0^η is equal to 0.467. From the fitting we obtain the values of A_η and E_η as 1.58 and 1.14, respectively.

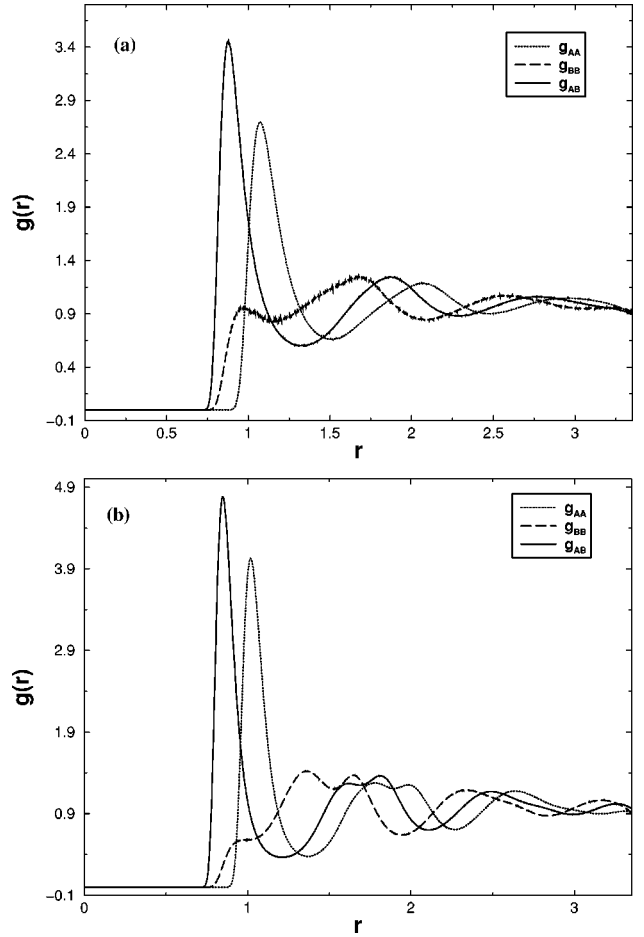


FIG. 1. Partial radial distribution functions plotted against distance at two different phase points. (a) $T^* = 1.0$ and $P^* = 2.5$ and (b) $T^* = 1.0$ and $P^* = 25.0$. Solid lines are g_{AB} , dotted lines are g_{AA} and dashed lines are g_{BB} . The strong attractive interaction between A and B particles is reflected in the highest peak value of g_{AB} and least interaction between the B particles is reflected in the smallest peak value of g_{BB} . In (b) the appearance of the split second peaks is due to random close packing.

Mode coupling theory predicts power law dependencies of the dynamic properties with temperature. We have tried to check the validity of MCT by fitting viscosity with the power law, $\eta = C_\eta (T - T_c^\eta)^{-\gamma_\eta}$. Figure 2(c) shows the plot of $\ln(\eta)$ against $\ln(T - T_c^\eta)$. MCT power law dependence of viscosity gives a poor fit in high temperature region. This was also observed by Michele *et al.*²⁷ So we fitted the power law dependence only upto $T^* = 1.0$. Critical temperature T_c^η predicted by MCT is 0.587 which is higher than the critical temperature T_0^η obtained from VFT fitting (0.467). So MCT power law actually predicts the divergence of viscosity much before the actual glass transition temperature and so it fails to describe transport in the very high viscosity region.

C. Pressure dependence of viscosity

The pressure dependence of the dynamical properties is found to be weaker than their temperature dependence. In Figs. 3(a) and 3(b), we have plotted $\ln(\eta)$ against pressure P^* for temperatures 1.0 and 0.5, respectively. In both cases,

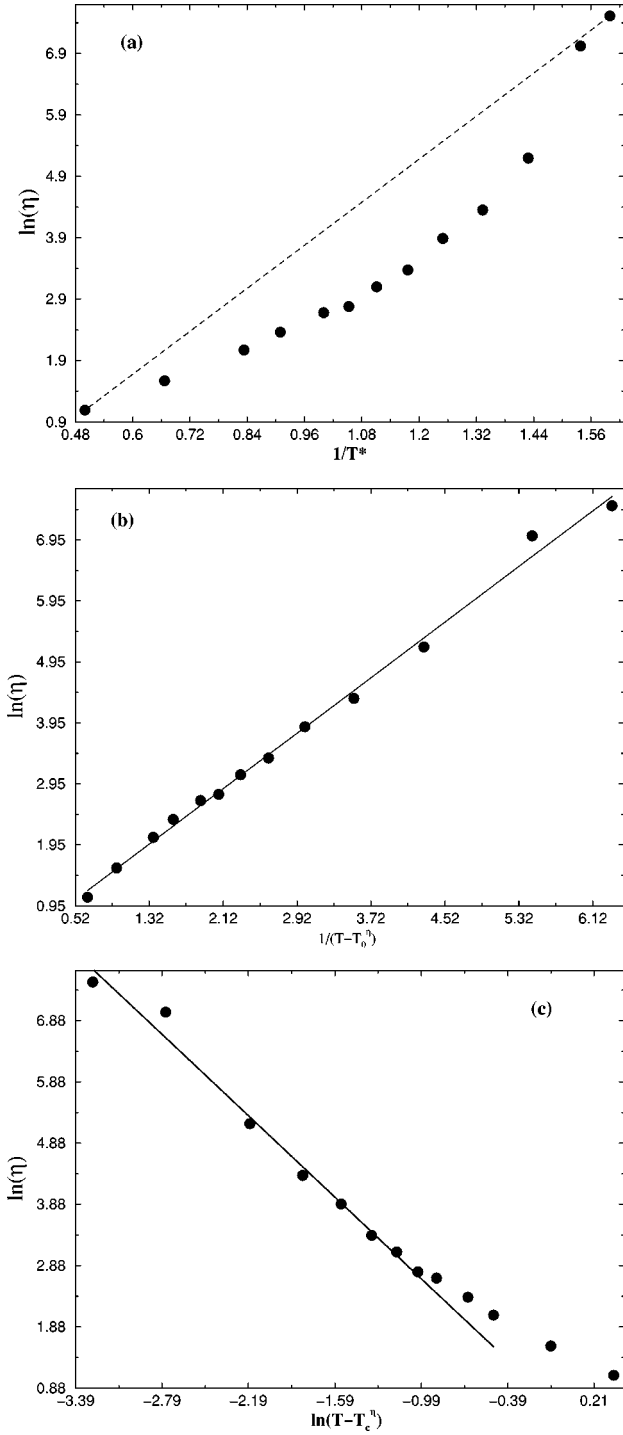


FIG. 2. Temperature dependence of viscosity at $P^* = 10$. (a) $\ln(\eta)$ is plotted against $1/T^*$. The simulated values given by the solid circles show super-Arrhenius behavior. The dotted line gives a guideline to the Arrhenius behavior. (b) $\ln(\eta)$ is plotted against $1/(T-T_0^\eta)$. Circles are simulation results and the solid line is the VFT fitting function. T_0^η is found to be 0.467. Slope (E_η) and intercept are 1.14 and 0.46, respectively. (c) Plot of $\ln \eta$ vs $\ln(T-T_c^\eta)$. Circles represent the simulation results and the solid line is the fit to the MCT power law. MCT critical temperature T_c^η is 0.587. The deviation of power law is clearly observed in high temperature region.

we find an Arrhenius or exponential dependence of viscosity on pressure. So, the functional form of pressure dependence of viscosity (η) can be written as

$$\eta = \alpha_\eta \times \exp[\lambda P^*]. \quad (8)$$

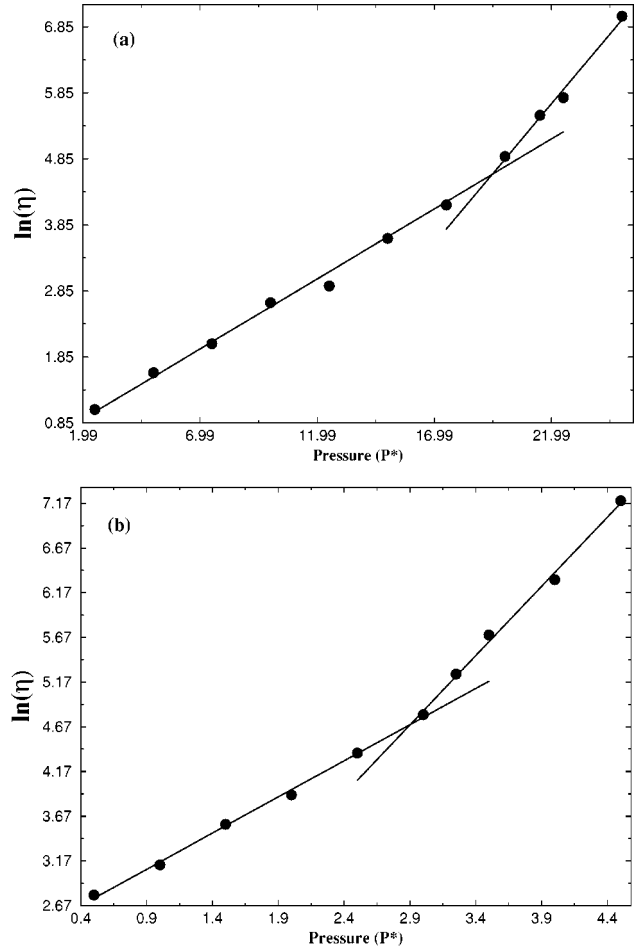


FIG. 3. Pressure dependence of viscosity. (a) $\ln \eta$ is plotted against pressure for $T^* = 1.0$. The circles are simulation results and the solid lines are fit to Arrhenius behavior. The change in slope takes place at around $P^* = 19.0$ and η approximately 80. (b) Similar plot as (a) for $T^* = 0.5$. Here the change in slope takes place at around $P^* = 3.0$ and η around 100.

The interesting fact to note here is that, for both the temperatures, there is a change in coefficient λ [consequently, a change in slope in Figs. 3(a) and 3(b)] after a certain high pressure which also depends upon the temperature of the system. For $T^* = 1.0$, λ changes from 0.21 to 0.42 while for $T^* = 0.5$, λ changes from 0.81 to 1.55. That is, at both the temperatures, the change in the strength of pressure dependence is significant, about a factor of 2. This may suggest a change in the mechanism of the stress relaxation. This can be associated with a crossover from a continuous, viscous mechanism of transport to a free energy landscape dominated transport. In fact, one can expect such a change also from the free volume theory.²⁸ We are not aware of any prior demonstration of this change in the pressure dependence of viscosity. As discussed later, we find a similar change in the pressure dependence of self-diffusion coefficients also (see later discussions).

D. Density variation of viscosity

It has been observed that the temperature dependence of viscosity is stronger than the pressure dependence.²⁹ In Fig. 4, $\ln \eta$ is plotted against number density (ρ) of the system.

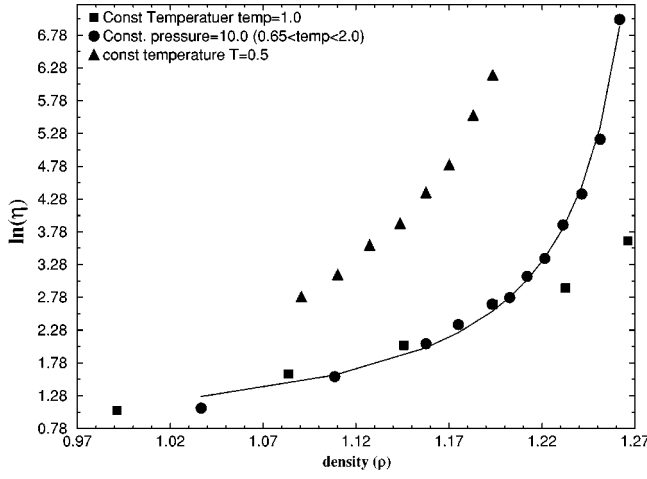


FIG. 4. Density dependence of viscosity. $\ln(\eta)$ is plotted against density ρ . Circles denote the simulation results where the density variation is obtained by changing temperature while keeping the pressure fixed at $P^* = 10.0$. Squares and triangles denote the simulation results where the variation in density is obtained by changing pressure while keeping the temperature fixed at $T^* = 1.0$ and 0.5 , respectively. Solid line is a fit of $\ln \eta$ against ρ to VFT type of equation.

Here density is changed by varying both temperature at fixed pressure 10.0 and varying pressure at fixed temperatures 1.0 and 0.5. Even at higher density, viscosity of the system is found to vary weakly with density at high temperature, whereas a sharp rise in viscosity with density is observed in the low temperature region, at a fixed pressure. We have analyzed trajectories for the system at two different thermodynamic state points ($T^* = 0.6$, $P^* = 10.0$ and $T^* = 1.0$, $P^* = 15.0$) with the same density ($\rho = 1.27$). While the low temperature system shows hopping mediated diffusion, the high T^* system shows mostly continuous diffusion, with occasional small jumps. Thus, the dynamics of the two systems are entirely different. The high T^* system seems to exhibit, even at such high density, normal liquidlike behavior. These results seem to show that the temperature is indeed the more dominant variable among the two parameters. This point has recently been discussed by Kivelson, Tarjus and co-workers²⁹ who suggested that the much stronger temperature dependence can be taken as an indication of the inadequacy of the mode coupling theory which is essentially based on a hard sphere model. This point needs further study.

E. Temperature dependence of diffusion coefficients

In the supercooled liquid, diffusion coefficients show non-Arrhenius temperature dependence which is of course well-known.^{6,10} However, we have calculated this dependence at different pressures. The results are depicted in Fig. 5(a) by plotting $\ln(D_i)$ against $1/T^*$. The curved figures signify that diffusion coefficients of this system follow super-Arrhenius behavior with temperature. So diffusion coefficients have been fitted to VFT type of equation as given by

$$D_i = A_{D_i} \times \exp[-E_{D_i}/(T - T_0^{D_i})], \quad (9)$$

where $T_0^{D_i}$ ($i = 1, 2$ signifies A, B type of particles) are the critical temperatures for diffusion coefficients.

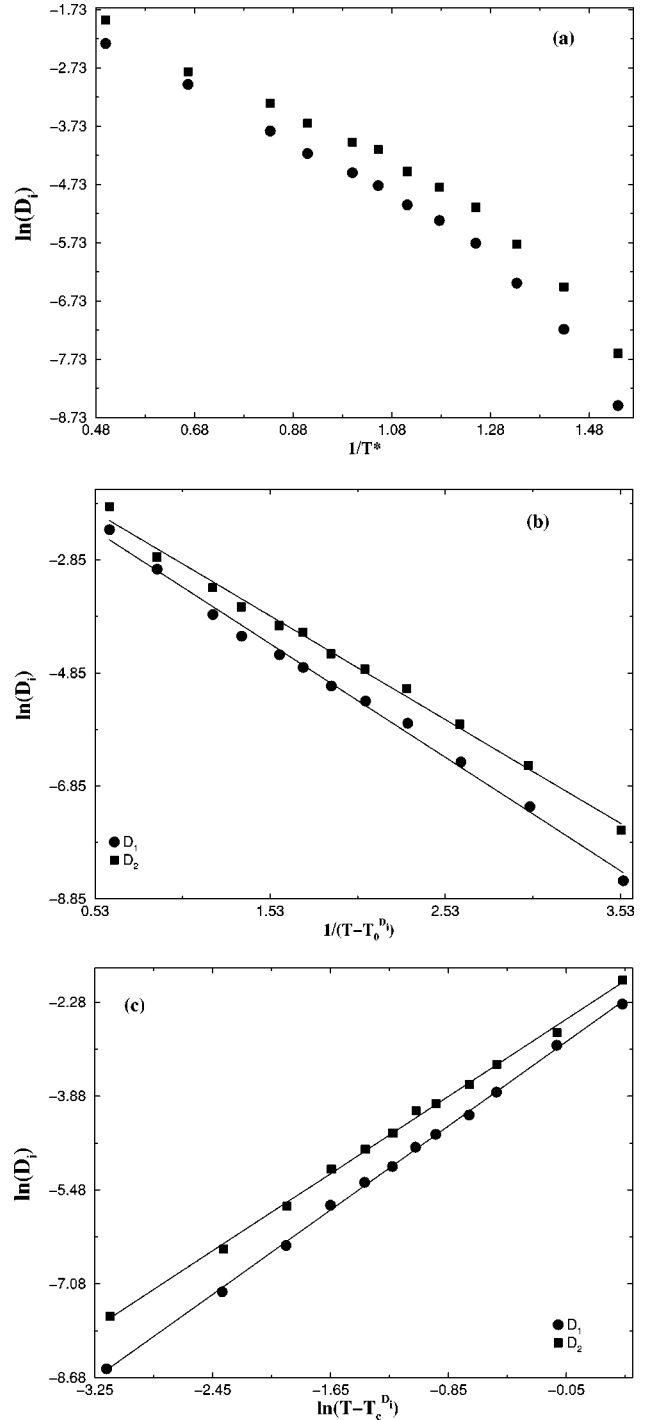


FIG. 5. Temperature dependence of diffusion coefficients. In each case below, circles and squares denote A and B particles, respectively. (a) $\ln D_i$ plotted against $1/T^*$ shows super-Arrhenius dependence of diffusion coefficients on temperature. (b) VFT fitting of diffusion coefficients. $\ln D_i$ is plotted against $1/(T - T_0^{D_i})$. Solid lines show the VFT fitting function. Critical temperature $T_0^{D_i}$ obtained from the fit is 0.368 for A and 0.367 for B type of particles. (c) Diffusion coefficients fitted to MCT equation. $\ln D_i$ is plotted against $\ln(T - T_c^{D_i})$. Solid lines show the MCT fitting function. Critical temperatures $T_c^{D_A}$ and $T_c^{D_B}$ are 0.608 and 0.607, respectively.

In Fig. 5(b), we plot $\ln(D_i)$ against $[1/(T - T_0^{D_i})]$ where $T_0^{D_A}$ and $T_0^{D_B}$ are 0.368 and 0.367, respectively. The critical temperatures obtained from diffusion coefficients ($T_0^{D_i}$) are less than the corresponding critical temperature obtained

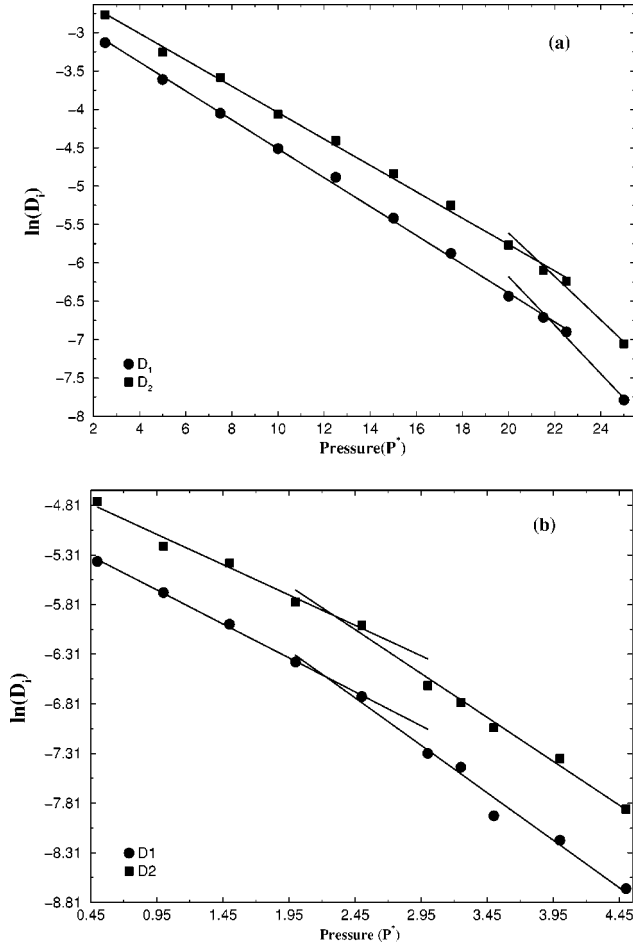


FIG. 6. Pressure dependence of diffusion coefficients. $\ln D_i$ is plotted against pressure P^* for (a) $T^* = 1.0$ and (b) $T^* = 0.5$. Circles and squares denote A and B particles, respectively. Solid lines represent the fitting to Arrhenius equation. (a) shows there is a change in slope at $P^* = 21.5$ while (b) shows the similar change in slope at $P^* = 3.0$.

from fitting viscosity values ($T_0^\eta = 0.467$). This signifies the decoupling of diffusion and viscosity in the proximity of glass transition and the breakdown of Stokes–Einstein law which support the fact that viscosity increases much faster than the decrease in diffusion coefficient.

Diffusion coefficients can also be well fitted to the MCT power law given by

$$D_i = C_{D_i} \times (T - T_c^{D_i})^\gamma, \quad (10)$$

where $T_c^{D_A}$ and $T_c^{D_B}$ are 0.608 and 0.607, respectively. $\ln D_i$ against $\ln(T - T_c^{D_i})$ is plotted in Fig. 5(c).

There are two points to note here. First, these transition temperatures from diffusion are higher than that obtained from fitting viscosity to MCT power law where the critical temperature is 0.587. Second, $T_c^{D_i}$'s are again significantly larger than the corresponding critical temperatures $T_0^{D_i}$ obtained from the fit to VFT type equation.

Another interesting observation is that the critical temperatures obtained from fitting to both MCT and VFT forms show higher transition values for the bigger particles than that for smaller particles, i.e., $T_0^{D_A}, T_c^{D_A} > T_0^{D_B}, T_c^{D_B}$. While this is consistent with the MCT prediction by Bosse *et al.*³⁰

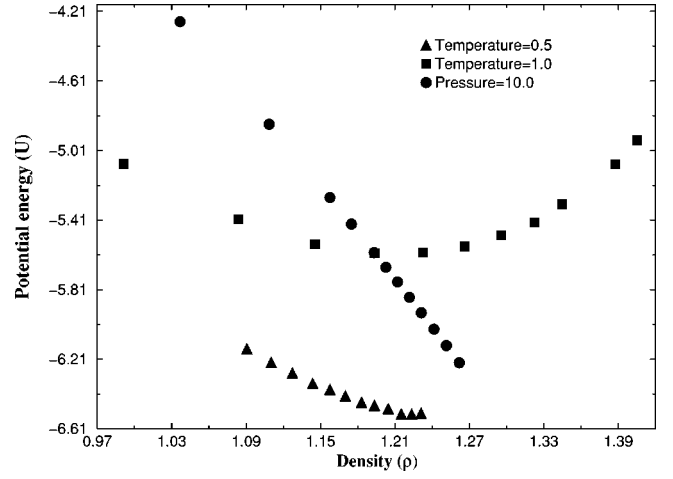


FIG. 7. Plot of potential energy U against density ρ . Circles show monotonic decrease of U with ρ , where ρ is varied by changing temperature and keeping the pressure fixed at $P^* = 10$. Squares and triangles denote the change in U against ρ where ρ is varied by changing pressure at a fixed temperature 1.0 and 0.5, respectively. We see a minimum in potential energy at a particular density when density is changed by varying pressure.

that, in a binary mixture, small particles can remain mobile when bigger particles have already stopped their motion, the difference we find between the two temperatures is rather small. This is not to be confused with the observation that the small ones remain more mobile even after the glass transition. But since the difference in the transition temperature is small, one can perhaps define a temperature range where the motion of both the particles undergo a qualitative change.

F. Pressure dependence of diffusion coefficients

Like the viscosity, the diffusion coefficients also show an exponential dependence on pressure. In Figs. 6(a) and 6(b), we plot $\ln D_i$ against pressure (P^*) at temperatures 1.0 and 0.5, respectively. Just as in viscosity, there is a change in the slope of Arrhenius dependence at a certain high pressure (see Fig. 3 for comparison). This crossover has been observed for both A and B type of particles and at both the two temperatures.

This change in the behavior of the transport properties takes place near a pressure where the hopping mode of transport also becomes noticeable. This may imply the emergence of free energy landscape dominated dynamics or may even signal the crossover predicted by the free volume theory. We have made several other studies to understand this behavior, as discussed below.

G. Variation of the total potential energy with density

Figure 7 shows the change in potential energy (U) against density when the latter is varied either by varying temperature at constant pressure or vice versa. U decreases linearly with density when the latter is changed by decreasing temperature at constant pressure, $P^* = 10.0$. However, the change in U by varying pressure shows a minimum at an intermediate density at a constant temperature (both for $T^* = 1.0$ and 0.5). So, even though with increasing pressure particles pack more densely, the system becomes energeti-

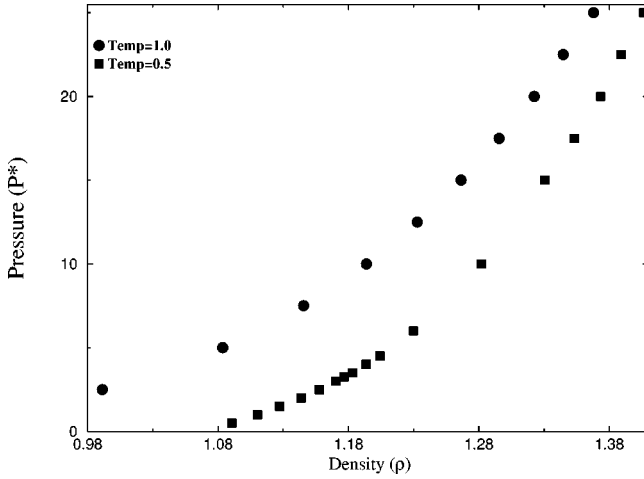


FIG. 8. Pressure (P^*) is plotted against density (ρ) for two different temperatures. Circles denote the values at $T^* = 1.0$ while squares denote those at $T^* = 0.5$.

cally frustrated after it reaches a certain density, even before the glass transition density. This is a curious result which may be of some relevance for glasses formed at high pressures.

H. Pressure variation with density

In order to pursue this inter-relationship between pressure, density and temperature, in Fig. 8 pressure (P^*) is plotted against density (ρ) for both $T^* = 1.0$ and 0.5. The dependence is clearly nonlinear. However, the change in pressure with density appears to be smooth and continuous. Thus, the sharp change observed in the pressure dependence of viscosity and self-diffusion is not reflected in the pressure-density graph. Thus, it appears that the change in the viscosity and self-diffusion is dynamic in origin.

IV. EMERGENCE OF THE HOPPING MODE OF MASS TRANSPORT

The relaxation of supercooled liquid is much more sluggish compared to normal liquid. But the emergence of hopping mode at supercooled liquid becomes a convenient relaxation channel for the system.^{22,31,32} Unlike normal liquid dynamics where molecular motion is regarded as continuous Brownian motion, there appears in the system a sudden, rather large, displacement of one or more particles in a very short duration of time. This is commonly known as hopping. In a deeply supercooled liquid, when a particle's motion is almost vibrational around a certain point in space, hopping seems to be the only relaxation mode. So the probability distribution of particle displacement becomes bimodal signifying two distinct dynamical behavior.

In Fig. 9(a), normalized distribution function $P_n(L, \tau) \times L^2$ for the smaller particles is plotted against displacement L for four different temperatures, T^* , varying from 1.0 to 0.6. Figure 9(b) shows the same for the bigger particles. Here $P_n(L, \tau)$ is defined as the normalized probability of displace-

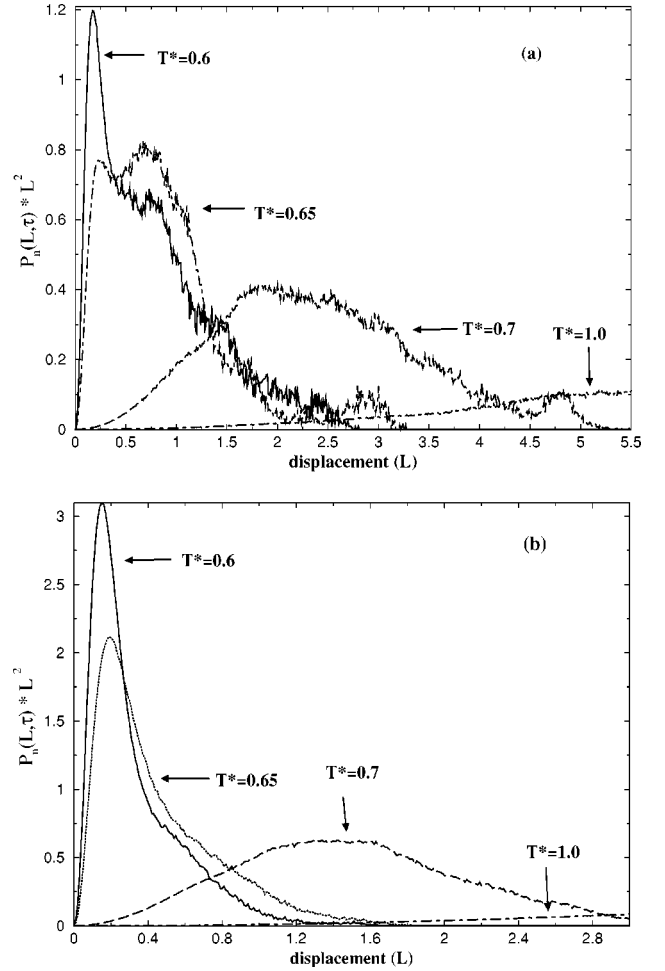


FIG. 9. Normalized probability distribution $P_n(L, \tau) \times L^2$ plotted against displacement L for different temperatures at a constant $P^* = 10.0$. The typical time window is 500τ . (a) Probability distributions for smaller (B) type of particles. (b) Same plot for the bigger particles (A). With decreasing temperature the probability distribution becomes bimodal for the smaller particles signifying the crossover from normal to hopping dominated dynamics.

ment of an n th particle between L and $L + dL$ after time τ from its original position at zero time. Note the emergence of bimodality at low temperatures.

Similarly, Figs. 10(a) and 10(b) show the distribution of $P_n(L, \tau) \times L^2$ against displacement L for smaller and bigger particles, respectively, at a constant temperature 0.5. Each figure contains results for different pressures. The typical time window taken in Figs. 9 and 10 is 500τ which is relatively large compared to the time scale of normal liquid. At low temperature and high pressure such as, $T^* = 0.6$ and $P^* = 25.0$, the sharp peak at $L = 0.2$ clearly signifies that the movement of particles in deep supercooled liquid is mostly vibrational in nature. On the other hand, for high temperature and low pressures, there is a significant amount of displacement observed for both types of particles. So, as expected, the continuous distribution at relatively low pressure and high temperature becomes clearly bimodal in nature at higher pressures and lower temperatures. This signifies the emergence of hopping dominated mass transfer from a continuous, viscosity dominated diffusion mode.

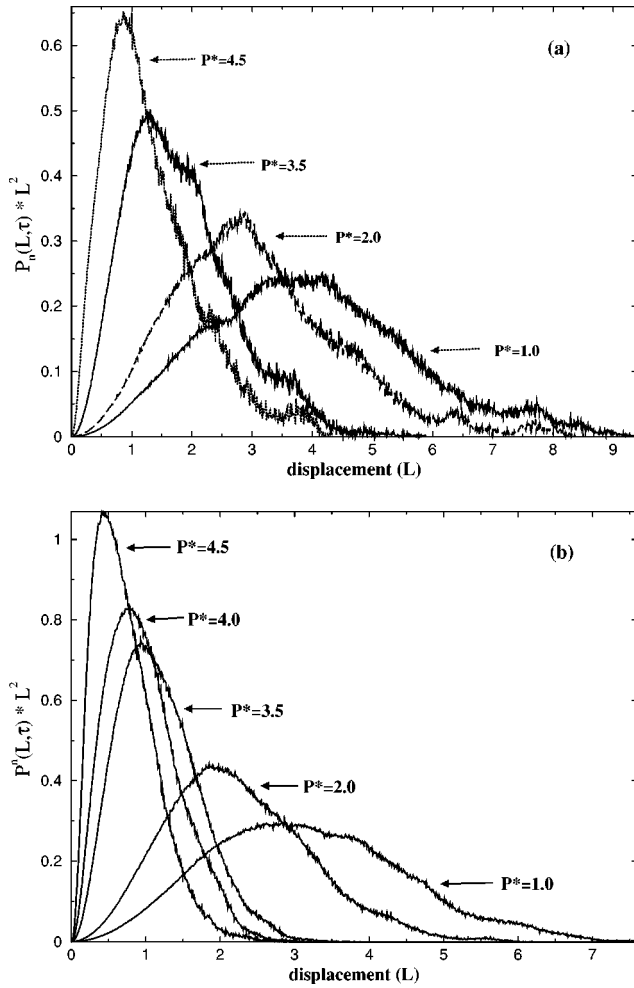


FIG. 10. Normalized probability distribution $P_n(L, \tau) \times L^2$ plotted against displacement L for different pressures at constant temperature $T^* = 0.5$. (a) Probability distribution for the smaller particles (B type). (b) Probability distribution for the bigger particles (A type). At high pressures, in case of smaller particles, the distribution becomes bimodal. Probability distribution of bigger particles does not show any significant bimodality.

Figures 11(a) and 11(b) depict the displacement trajectory of a small particle at $T^* = 0.6$, $P^* = 10.0$ and $T^* = 0.5$, $P^* = 4.5$, respectively. The displacement shows continuous movement as well as a sudden hopping. The two figures show two different kinds of hopping. As mentioned earlier, hopping of small particles continue to be rather frequent even in the deeply supercooled liquid.

Note that sometimes hopping has been used to determine the glass transition temperature. The present simulations, on the other hand, show that *the glass transition temperatures obtained from fitting to viscosity and diffusion are substantially lower than the temperatures where hopping is noticeable*. The present study thus seems to show that the emergence of hopping may occur substantially before the glass transition temperature.

The hopping may have significance in determining the fragility of a liquid.⁴ It is obvious that if the hopping mode can contribute substantially to diffusion and stress relaxation, then the temperature dependent studies may reveal an exponential temperature dependence. The fact that the Kob-Andersen model is weakly fragile is consistent with the

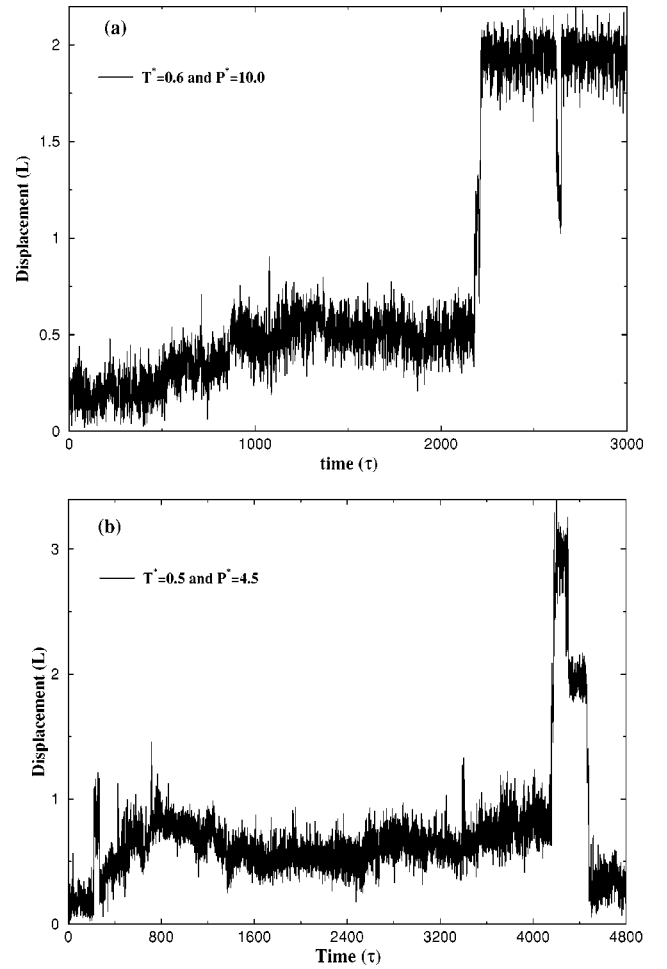


FIG. 11. Displacement of a small B type of particle is plotted against time τ at (a) $P^* = 10.0$ and $T^* = 0.6$ and at (b) $P^* = 4.5$ and $T^* = 0.5$. Sudden large displacement in each case is characterized as hopping.

emergence of hopping in this system before the glass transition temperature. We should state here that we are using the word “hopping mode” to describe collectively all the hopping—it is not meant to imply a true existence of a well-defined mode, like in hydrodynamics.

V. NONEXPONENTIAL STRESS RELAXATION

The slowing down of the dynamics in a supercooled liquid is reflected not only in the dynamic structure factor (which is commonly computed in simulations) but also in the shear stress relaxation, $\eta(t)$. The latter is a much more difficult quantity to obtain via simulations. According to MCT, $\eta(t)$ has a short time (binary contribution) and a long time (density mode contribution) part. On increasing the degree of supercooling (either by increasing pressure or by decreasing temperature), the decay of the stress correlation function in the long time part changes from an exponential to a stretched exponential (nonexponential) and in the regime closer to glass transition, the stress, at intermediate times, is predicted to relax by a power law. Stress time correlation function has been monitored in the present model for different pressures and temperatures. We have used all three different off-diagonal stress tensors [see Eq. (1)] to calculate the average

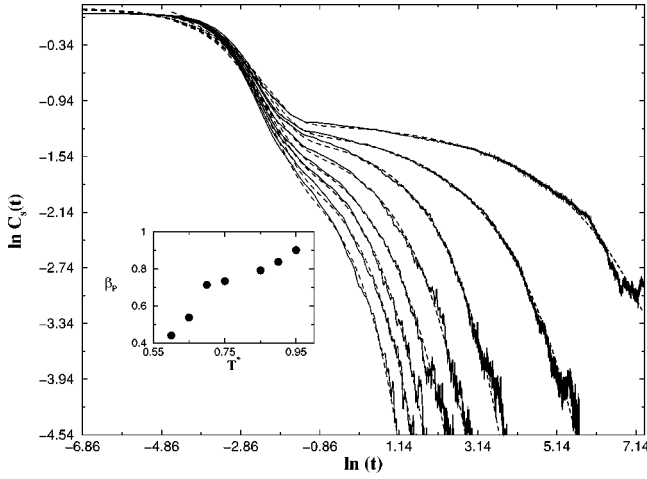


FIG. 12. Solid lines represent the $\ln C_s(t)$ vs $\ln(t)$ plots for $T^* = 0.6$ to 0.95 at a constant $P^* = 10.0$. $C_s(t)$ shows an increasing nonexponentiality as the temperature is decreased. Dashed lines in each case are the plot of the fitting function [see Eq. (11)]. The temperature dependence of the stretching parameter β_p [as obtained from the fitting to the Eq. (11)] at constant $P^* = 10.0$ is shown in the inset.

stress time correlation function. Viscosity η has also been calculated from the average stress correlation function. It is well known that there is much more uncertainty or error involved in the calculation of viscosity from stress correlation in the supercooled region.³¹ It has also been observed that unlike in normal liquid, in supercooled liquid the three different stress correlation functions (xy, yz, xz) become anisotropic, within the time window of the simulations. In Fig. 12, the log of normalized stress autocorrelation functions [$\ln C_s(t)$] are plotted against log of time [$\ln(t)$] for eight different temperatures from 0.6 to 0.95 at a constant pressure 10.0. Similarly in Fig. 13, $\ln C_s(t)$ is plotted against $\ln(t)$ for six different pressures from 5.0 to 25.0 at a constant temperature 1.0. Then $C_s(t)$ has been fitted to the equation given below:

$$C_s(t) = A \exp(-t/\tau_1) + B \exp[-(t/\tau)^\beta]. \quad (11)$$

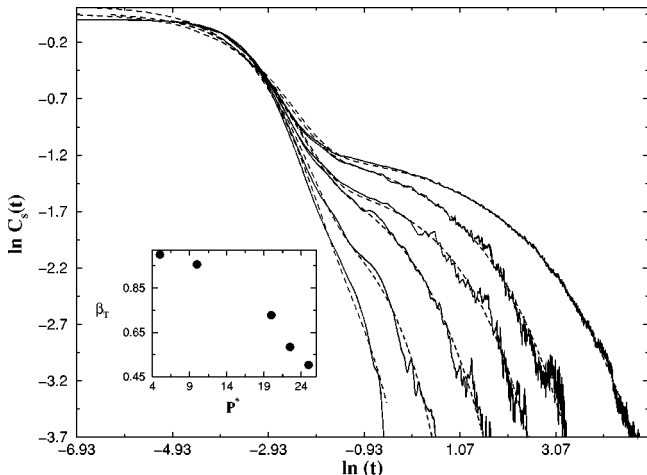


FIG. 13. Solid lines show the $\ln C_s(t)$ vs $\ln(t)$ plots for $P^* = 5.0$ to 25.0 at constant $T^* = 1.0$. Dashed lines in each case are the plots of the fitting function [see Eq. (11)]. The pressure dependence of stretching parameter β_T at constant $T^* = 1.0$ is shown in the inset.

The term proportional to A takes into account of the fast decay and the term proportional to B determines the slow exponential decay in normal liquid which changes to a stretched exponential form in the supercooled liquid. We found that the stretching parameter β decreases from 1.0 to about 0.44 as the liquid is changed from normal to deeply supercooled liquid. Note that the above functional form is not suitable to describe the real short time (ballistic, inertial) dynamics, but that is no limitation in the present case as we are interested mainly in the longer time aspects of relaxation. The characteristic time of the fast decay τ_1 is almost constant in each of the cases, i.e., it is independent of temperature and pressure.

The insets in Figs. 12 and 13 show the dependence of β on temperature and on pressure, respectively. The stretching parameter β has been calculated by fitting the stress correlation to the above function. Similar type of temperature dependence of normalized stress correlation has been discussed recently.³³ β varies from 0.44 to 1.0 as expected in theories and simulations.^{34,35}

Stress correlation functions are often fitted to the power law behavior predicted by the ideal mode coupling theory.^{36,37} Decay of the stress correlation function depicted in Fig. 12 ($P^* = 10$) for the lowest temperature ($T^* = 0.6$) clearly shows the emergence of the power law at the intermediate time. The long time part of it has been fitted to Von Schweidler power law [$\eta = f - h(t/\tau)^{\beta_{PL}}$]. The exponent β_{PL} is found to be 0.22 for this case ($T^* = 0.6$ and $P^* = 10.0$). However, this seems to be just the beginning of the power law in the sense that one needs to go to even lower temperatures to recover the full power law behavior. We have not been able to go down to any lower temperatures. Even at $T^* = 0.6$, $P^* = 10$, we needed to simulate over 15 million steps and average over three runs to get reliable statistics. We estimate that the computation cost will increase by at least one order of magnitude (or more) to lower the temperature even by 0.02.

The emergence of the power law with such a small exponent implies the existence of a large separation of time scale between the initial fast decay and the very slow long time decay. Since the time scale of the initial decay is less than a picosecond (if we may use the parameters for argon), this is clearly related to the relaxation in the cage which contributes, in this case, about 70% of the total stress relaxation. The power law part contributes less than 10%. The main point here is that the emergence of power law requires the establishment of a large separation of time scale between the two main relaxation mechanisms. The two relevant points here are the role of particle hopping and the fragility of the liquid. For more fragile liquid, the separation of time scale should be larger, giving rise to power law decay with smaller exponent, and also, less frequency of hopping. We are not aware of any study correlating these factors.

VI. CONCLUSION

Understanding the dynamics of supercooled liquid is still a challenge to theoreticians. This problem has remained

largely misunderstood, despite considerable efforts in recent years which nevertheless has augmented our understanding a great deal.

In this work, we presented results of a large number of simulations of a glassy binary mixture, with an emphasis on the pressure dependence of the static and dynamic properties. The aim has been to characterize the behavior of liquid ranging from normal to supercooled region. The Kob–Andersen model has been used as the probe of the study as it is well known for a good glass former. Moreover, the model contains disparate sized and differently interacting particles which allow for many interesting dynamical behavior of the two particles.

The present study revealed several interesting results, prominent among them is the change in the pressure dependence of viscosity and self-diffusion coefficients and the demonstration that the temperature has a much stronger effect than density in controlling the dynamical properties of the supercooled liquid. Several other results, like the decoupling between viscosity and self-diffusion and the higher transition temperature prediction by the mode coupling theory, are known from earlier studies.

The observed sharp change in the pressure dependence of viscosity and diffusion coefficients seems to indicate a change in the mechanism of transport properties in viscous liquids. This change occurs at a pressure where the hopping of particles becomes noticeable. However, the change can also be explained from the free volume theory which envisages such a change in the transport scenario, arising from the random close packing at very high density. Unfortunately, we have not been able to provide any discriminatory evidence in favor of one or the other of these two alternatives.

ACKNOWLEDGMENTS

It is a pleasure to thank Professor Srikanth Sastry and Professor Chandan Dasgupta for discussions and help and for bringing several useful references to our attention. A.M. thanks Jean Francois Dufreche, Kausik Chakraborty, and Goundla Srinivas for helpful suggestions, help and discussions. This work has been supported by grant from the Council of Scientific and Industrial Research, India.

- ¹ See papers in *J. Phys.: Condens. Matter* **12** (2000).
- ² W. Gotze, in *Liquid, Freezing and the Glass Transition*, edited by D. Levesque, J. P. Hansen, and J. Zinn-Justin (North-Holland, Amsterdam, 1990).
- ³ G. Adam and J. H. Gibbs, *J. Chem. Phys.* **43**, 139 (1965).
- ⁴ T. S. Grigera, A. Cavagna, I. Giardina, and G. Parisi, cond-mat/0107198 v 1, 10 July 2001.
- ⁵ B. Bagchi, *J. Chem. Phys.* **101**, 9946 (1994).
- ⁶ S. Sastry, *Nature (London)* **409**, 164 (2001).
- ⁷ W. Kob and H. C. Andersen, *Phys. Rev. E* **51**, 4626 (1995).
- ⁸ W. Kob and H. C. Andersen, *Phys. Rev. Lett.* **73**, 1376 (1994).
- ⁹ S. Sastry, P. G. Debenedetti, and F. H. Stillinger, *Nature (London)* **393**, 554 (1998).
- ¹⁰ S. Sastry, *Phys. Rev. Lett.* **85**, 590 (2000).
- ¹¹ K. Vollmayr, W. Kob, and K. Binder, *J. Chem. Phys.* **105**, 4714 (1996).
- ¹² F. Sciortino, W. Kob, and P. Tartaglia, *Phys. Rev. Lett.* **83**, 3214 (1999).
- ¹³ B. Coluzzi, G. Parisi, and P. Verrocchio, *J. Chem. Phys.* **112**, 2933 (2000).
- ¹⁴ C. A. Angell, *J. Non-Cryst. Solids* **131–133**, 13 (1991).
- ¹⁵ M. T. Cicerone and M. D. Ediger, *J. Chem. Phys.* **104**, 7210 (1996).
- ¹⁶ J. A. Hodgdon and F. H. Stillinger, *Phys. Rev. E* **48**, 207 (1993).
- ¹⁷ F. H. Stillinger and J. A. Hodgdon, *Phys. Rev. E* **50**, 2064 (1994).
- ¹⁸ M. T. Cicerone, P. A. Wagner, and M. D. Ediger, *J. Phys. Chem. B* **101**, 8727 (1997).
- ¹⁹ R. Zwanzig, *Annu. Rev. Phys. Chem.* **16**, 67 (1965).
- ²⁰ R. Zwanzig and R. D. Mountain, *J. Chem. Phys.* **43**, 4464 (1965).
- ²¹ D. A. McQuarrie, *Statistical Mechanics* (Harper and Row, New York, 1976).
- ²² G. Wahnström, *Phys. Rev. A* **44**, 3752 (1991).
- ²³ D. Brown and J. H. R. Clarke, *Mol. Phys.* **51**, 243 (1984).
- ²⁴ H. C. Andersen, *J. Chem. Phys.* **72**, 2384 (1980).
- ²⁵ J. M. Haile and H. W. Graben, *J. Chem. Phys.* **73**, 2412 (1980).
- ²⁶ S. D. Stoddard and J. Ford, *Phys. Rev. A* **8**, 1504 (1973).
- ²⁷ C. D. Michele and D. Leporini, *Phys. Rev. E* **63**, 036701 (2001).
- ²⁸ D. Turnbull and M. H. Cohen, *J. Chem. Phys.* **31**, 1164 (1959).
- ²⁹ G. Tarjus, D. Kivelson, and P. Viot, *J. Phys.: Condens. Matter* **12**, 6497 (2001).
- ³⁰ J. Bosse and Y. Kaneko, *Phys. Rev. Lett.* **74**, 4023 (1995).
- ³¹ J.-L. Barrat, J.-N. Roux, and J.-P. Hansen, *Chem. Phys.* **149**, 197 (1990).
- ³² J.-N. Roux, J.-L. Barrat, and J.-P. Hansen, *J. Phys.: Condens. Matter* **1**, 7171 (1989).
- ³³ L. Angelani, G. Parisi, G. Ruocco, and G. Vilianni, *Phys. Rev. Lett.* **81**, 4648 (1998).
- ³⁴ M. T. Cicerone, F. R. Blackburn, and M. D. Ediger, *J. Chem. Phys.* **102**, 471 (1995).
- ³⁵ I. A. Campbell, J. M. Flesselles, R. Jullien, and R. Botet, *Phys. Rev. B* **37**, 3825 (1988).
- ³⁶ G. Hinze, D. D. Brace, S. D. Gottke, and M. D. Fayer, *J. Chem. Phys.* **113**, 3723 (2000).
- ³⁷ G. Hinze, D. D. Brace, S. D. Gottke, and M. D. Fayer, *Phys. Rev. Lett.* **84**, 2437 (2000).